

## Probing the $WWZ$ vertex at a $\sqrt{s} = 500$ GeV $e^+e^-$ collider

Gilles Couture

*Physics Department, Southern Methodist University, Dallas, Texas 75275*

Stephen Godfrey

*Ottawa-Carleton Institute for Physics, Department of Physics, Carleton University, Ottawa, Canada K1S 5B6*

Randy Lewis

*Department of Physics, University of Toronto, Toronto, Canada M5S 1A7*

(Received 23 July 1991)

We study the precision measurement of the  $WWZ^0$  vertex in the process  $e^+e^- \rightarrow \nu\bar{\nu}\mu^+\mu^-$  at a  $\sqrt{s} = 500$  GeV  $e^+e^-$  collider. We find that this process can be used to make a precise determination of the trilinear gauge boson couplings. Assuming an integrated luminosity of  $2 \text{ fb}^{-1}$ , in the reaction  $e^+e^- \rightarrow \nu\bar{\nu}\mu^+\mu^-$ ,  $\kappa_Z$  can be measured to 10% at the 95% C.L. and  $\lambda_Z$  to  $\pm 0.07$  at 95% C.L. With the appropriate cuts on  $M_{\mu^+\mu^-}$ ,  $\Delta\kappa_Z = {}^{+0.3}_{-0.4}$  and  $\Delta\lambda_Z = {}^{+0.4}_{-0.6}$  at 95% C.L. independent of deviations in  $\kappa_\gamma$  and  $\lambda_\gamma$ .

PACS number(s): 13.10.+q, 12.15.Ji, 13.40.Fn, 14.80.Er

### I. INTRODUCTION

The standard model of the electroweak interactions [1] is consistent with all experimental measurements [2]. Although the fermion-gauge-boson sector of the theory is being tested to ever increasing precision [3]; the gauge boson couplings have yet to be subjected to stringent direct experimental measurements. At present, crude constraints exist on the  $WW\gamma$  couplings from  $W\gamma$  production in  $p\bar{p}$  collisions at the Fermilab  $p\bar{p}$  collider Tevatron [4] and in the near future, measurement of the  $\gamma WW$  vertex will be possible at the DESY  $ep$  collider HERA through single  $W$  production [5] and high  $p_T$  photons [6]. Statistics will be the main limiting factor and will not allow a measurement better than 50%. Soon afterwards, the CERN  $e^+e^-$  collider LEP 200 will study both the  $WW\gamma$  and  $WWZ^0$  couplings through  $W$  pair production:  $e^+e^- \rightarrow W^+W^-$  [7]. A drawback of this process is that both vertices contribute roughly equally to the  $W$  pair production cross section because the photon and the  $Z$  boson are both far off mass shell. This implies that only a linear combination of the two vertices will effectively be measured. It is therefore important that independent measurements of these couplings be made in order to complement the LEP 200 analysis. In this paper we study the sensitivity of the process  $e^+e^- \rightarrow \nu\bar{\nu}Z^0$  to anomalous couplings of the  $WWZ^0$  vertex, which can be studied at the "Next Linear Collider" (NLC): an  $e^+e^-$  collider with  $\sqrt{s} = 500$  GeV or more [8,9].

### II. THE $WWZ^0$ VERTEX

Within the standard model, the  $WW\gamma$  and  $WWZ$  vertices are uniquely determined by  $SU(2)_L \times U(1)$  gauge invariance so that a precise measurement of the vertices comprises a stringent test of the gauge structure of the theory. The most general Lorentz and  $CP$ -invariant

$WWV$  vertex compatible with electromagnetic gauge invariance is customarily parametrized as [10]

$$\mathcal{L}_{\text{eff}} = -ig_V \left\{ (W_{\mu\nu}^\dagger W^\mu V^\nu - W_\mu^\dagger V_\nu W^{\mu\nu}) + \kappa_V W_\mu^\dagger W_\nu F^{\mu\nu} + \frac{\lambda_V}{M_W^2} W_{\lambda\mu}^\dagger W_\nu^\mu F^{\nu\lambda} \right\}, \quad (1)$$

where  $V$  represents either the photon or  $Z^0$  and  $W^\mu$ , represents the  $W^-$  fields, and where  $g_\gamma = e$  and  $g_{Z^0} = e \cot d_W$ . As usual,  $W_{\mu\nu} = \partial_\mu W_\nu - \partial_\nu W_\mu$  and  $F_{\mu\nu} = \partial_\mu V_\nu - \partial_\nu V_\mu$  denote the  $W$  and photon (or  $Z^0$ ) field-strength tensors. We note that the presence of the  $W$ -boson mass in the  $\lambda_V$  term is *ad hoc* and one could argue that a scale for new physics ( $\Lambda$ ) of several TeV's is more appropriate than this much smaller energy scale. We will conform to the customary parametrization and will not address this issue further.

In the static limit, the parameters  $\kappa_\gamma$  and  $\lambda_\gamma$  are related to the anomalous magnetic dipole moment ( $\mu_W$ ) and the electric quadrupole moment ( $Q_W$ ) of the  $W$  by

$$\mu_W = \frac{e}{2M_W} (1 + \kappa_\gamma + \lambda_\gamma), \quad Q_W = -\frac{e}{M_W^2} (\kappa_\gamma - \lambda_\gamma) \quad (2)$$

with similar relations for the  $WWZ^0$  vertex. At tree level the standard model predicts  $\kappa_V = 1$  and  $\lambda_V = 0$ . Higher order corrections to  $\mu_W$  and  $Q_W$  have been calculated [11] and the results are in the 2% range in the minimal standard model and in the 3% range in supersymmetric models [12].

In composite models, however, all four parameters are essentially free. One must rely, for example, on unitarity [13] or experimental observables such as  $(g-2)_\mu$  [14], the masses of the gauge bosons [15], and the partial widths of the  $Z$  boson [16] to constrain the parameters.

### III. THE PROCESS $e^+e^- \rightarrow \nu\bar{\nu}\mu^+\mu^-$

The process  $e^+e^- \rightarrow \nu\bar{\nu}\mu^+\mu^-$  offers the possibility of measuring the  $WWZ^0$  vertex without interference from the  $WW\gamma$  vertex by making appropriate kinematic cuts on the  $\mu^+\mu^-$  invariant mass. In total, there are 28 distinct Feynman diagrams which contribute to the process  $e^+e^- \rightarrow \nu\bar{\nu}\mu^+\mu^-$  of which we are interested in only one; the  $W^+W^-$  fusion to a  $Z^0$  boson followed by the decay  $Z^0 \rightarrow \mu^+\mu^-$ , which is shown in Fig. 1. Nevertheless, to properly take into account the nonresonant background and maintain gauge invariance our calculation includes all diagrams for arbitrary values of  $\kappa_V$  and  $\lambda_V$ , where  $V$  denotes either  $\gamma$  or  $Z^0$ .

To evaluate the cross sections and distributions we used the CALKUL helicity amplitude technique [17] to obtain expressions for the matrix elements and used Monte Carlo techniques to perform the phase-space integration [18]. In our results we take  $\alpha=1/128$ ,  $\sin^2\theta_W=0.23$ ,  $M_Z=91.172$  GeV,  $\Gamma_Z=2.5$  GeV,  $M_W=81.0$  GeV, and  $\Gamma_W=2.1$  GeV.

The signal we are considering consists of an energetic  $\mu^+\mu^-$  pair plus missing transverse momentum  $\cancel{p}_T$  due to the neutrinos coming from the original beam electron and positron. We require  $\cancel{p}_T > 10$  GeV. This eliminates the potential background of  $e^+e^- \rightarrow e^+e^-\mu^+\mu^-$  via two photons where the  $e^+$  and  $e^-$  escape down the beam pipe. In addition we require that  $E_{\mu^\pm} > 10$  GeV and to take into account detector acceptance we require that the  $\mu^+$  and  $\mu^-$  be at least  $10^\circ$  from the beam line. Our conclusions are not sensitive to the exact values of these cuts. In Fig. 2 we show the cross section for  $e^+e^- \rightarrow \nu\bar{\nu}\mu^+\mu^-$  as a function of  $\sqrt{s}$  for the above cuts and for several different cuts on the  $\mu^+\mu^-$  invariant mass ( $M_{\mu^+\mu^-}$ ). We note that the cross section does not go down as does the QED point cross section  $\sigma(e^+e^- \rightarrow \mu^+\mu^-)$  for the energy range under consideration so one gains by going to higher  $\sqrt{s}$ . In the remainder of this paper we will concentrate on the NLC  $e^+e^-$  collider machine parameters of  $\sqrt{s}=500$  GeV,  $\mathcal{L}=10^{32}\text{cm}^{-2}\text{sec}^{-1}$  yielding a yearly integrated luminosity of  $L=2$  fb $^{-1}$  (which results in of order 1000 events/yr for each unit of  $R=4\pi\alpha^2/3s$ , the point cross section).

The cross section for no cuts on  $M_{\mu^+\mu^-}$  (solid line) is considerable as it is dominated by low-invariant-mass events due to the photon pole which appears in many of

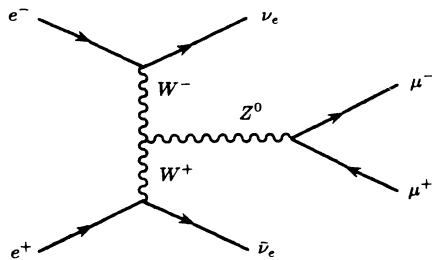


FIG. 1. Feynman diagram for the process  $e^+e^- \rightarrow \nu\bar{\nu}Z^0$  followed by  $Z^0 \rightarrow \mu^+\mu^-$ , which includes the  $WWZ^0$  vertex.

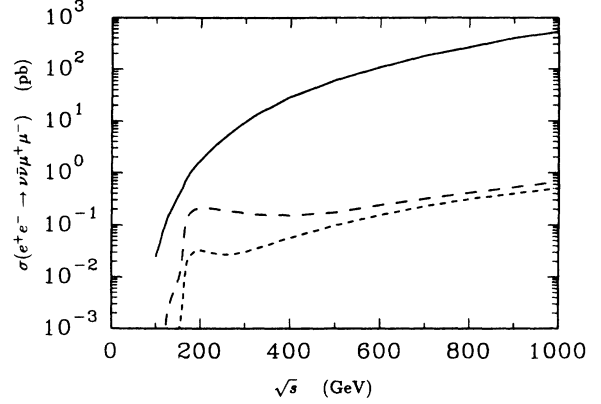


FIG. 2.  $\sigma(e^+e^- \rightarrow \nu\bar{\nu}\mu^+\mu^-)$  as a function of  $\sqrt{s}$  for  $\theta_{\mu^\pm} > 10^\circ$ . The solid line is for no cut on  $M_{\mu^+\mu^-}$ , the long-dashed line for  $M_{\mu^+\mu^-} > 25$  GeV, and the short-dashed line for  $86 \text{ GeV} < M_{\mu^+\mu^-} < 96 \text{ GeV}$ .

the Feynman diagrams, including photon bremsstrahlung and the diagram of Fig. 1 with the  $Z^0$  replaced by a photon. Imposing a cut  $M_{\mu^+\mu^-} > 25$  GeV eliminates this pole and reduces the cross section substantially (long-dashed line). Finally, if we impose the cut that  $M_{\mu^+\mu^-}$  lies within 5 GeV of the  $Z$  pole (short-dashed line) we can separate the effects of the  $WWZ^0$  from those of the  $WW\gamma$  vertex on the cross section. We verified that with this last cut on the invariant mass of the lepton pair, the cross section is insensitive ( $\sigma$  varies by less than 1%) to variations in  $\kappa_\gamma$  and  $\lambda_\gamma$  of  $\pm 0.2$  around their standard model (SM) values while varying  $\kappa_z$  from  $-2$  to  $1.5$  and  $\lambda_z$  from  $-1$  to  $1$ . Furthermore, the different distributions that we used remained unchanged by these variations in the photon parameters. For larger variations in the photon sector, the cross section varies by less than 2% and 6% for variations of  $\pm 0.5$  in  $\kappa_\gamma$  and  $\lambda_\gamma$ , respectively. As a point of reference, the statistical error for 2

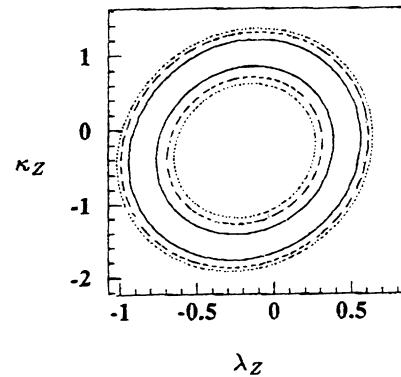


FIG. 3. Confidence level contours for consistency of the cross section  $\sigma(e^+e^- \rightarrow \mu^+\mu^-\nu\bar{\nu})$  with the standard-model prediction as a function of  $\kappa_z$  and  $\lambda_z$  using the cuts described in the text. The solid line is the 68% C.L., the dashed line is the 90% C.L., and the dotted line is the 95% C.L.

$\text{fb}^{-1}$  integrated luminosity corresponds to an uncertainty in  $\sigma$  of roughly 7% so that at the  $1\sigma$  level the process at hand is insensitive to variations in  $\kappa_\gamma$  and  $\lambda_\gamma$  of  $\pm 0.5$ .

Our interest in this process is to see how precisely  $\kappa_Z$  and  $\lambda_Z$  can be measured as a test of the gauge structure of the standard model. We therefore impose the cut  $86 \text{ GeV} < M_{\mu^+\mu^-} < 96 \text{ GeV}$ . To quantify the sensitivity to  $\kappa_Z$  and  $\lambda_Z$  we begin by considering the effect of varying  $\kappa_Z$  and  $\lambda_Z$  on the cross section  $\sigma(e^+e^- \rightarrow \mu^+\mu^-\nu\bar{\nu})$  with the cuts described above. We test for consistency with the standard model based on the statistical errors expected from integrated luminosities of 2 and  $5 \text{ fb}^{-1}$ . In Fig. 3 we show 68%, 90%, and 95% confidence level contours for consistency with the standard model in the  $\kappa_Z$ - $\lambda_Z$  plane based on  $2 \text{ fb}^{-1}$  integrated luminosity. The region between the rings is consistent with the standard model. Note that there are regions in the parameter space which deviate substantially from the standard model but have cross sections which are consistent with that of the standard model. Varying one parameter at a time we find  $\Delta\kappa_Z = {}^{+0.3}_{-0.4}$  ( $\lambda_Z = 0$ ) and  $\Delta\lambda_Z = {}^{+0.4}_{-0.6}$  ( $\kappa_Z = 1.0$ ), which gives a much different picture of the allowed parameter space. This underlines the importance of performing a global analysis of all free parameters to obtain a realistic test of the theory and the pitfalls of varying one parameter at a time.

Fortunately, there is more information available beyond the cross-section measurement. We analyzed numerous distributions of kinematic variables and found that the angular distribution of the outgoing muons with respect to each other ( $\theta_{\mu^+\mu^-}$ ) and the  $p_T$  distribution of the  $Z$  are particularly sensitive to anomalous couplings. In Figs. 4(a) and 4(b) we show the angular distributions and  $p_{TZ}$  distributions, respectively, for several representative values of  $\kappa_Z$  and  $\lambda_Z$  which in Fig. 3 appeared to be consistent with the standard model on the basis of the cross section measurement. One clearly sees that the angular distributions and  $p_{TZ}$  distributions for those values of  $\kappa_Z$  and  $\lambda_Z$  are substantially different. To quantify this we divide the angular distribution into 3 regions:  $-1.0 < \theta_{\mu^+\mu^-} < -0.5$ ,  $-0.5 < \theta_{\mu^+\mu^-} < -0.1$ , and  $-0.1 < \theta_{\mu^+\mu^-} < 0.75$  and perform a  $\chi^2$  analysis. The 68%, 90%, and 95% confidence level contours are shown in Figs. 5(a) and 5(b) based on 2 and  $5 \text{ fb}^{-1}$  integrated luminosity, respectively. Similarly, we divided the  $p_{TZ}$  distribution into three bins:  $p_{TZ} < 80 \text{ GeV}$ ,  $80 \text{ GeV} < p_{TZ} < 120 \text{ GeV}$  and  $120 \text{ GeV} < p_{TZ} < 240 \text{ GeV}$ . The 68%, 90%, and 95% confidence level bounds are shown in Figs. 5(c) and 5(d) for integrated luminosities of 2 and  $5 \text{ fb}^{-1}$ , respectively. This additional information from the distributions substantially restricts the allowed region in parameter space that is consistent with the standard model. Varying one parameter at a time leads roughly to  $0.4 < \kappa_Z < 1.5$  and  $-0.6 < \lambda_Z < 0.5$  (95% C.L. and using  $2 \text{ fb}^{-1}$ ), it is clear from these figures that the realistic limits are broader:  $\kappa_Z$  extends from 0 to 1.5 and  $\lambda_Z$  from  $-0.6$  to 0.5.

With real data one would likely do better in the sense that rather than utilizing general binnings of the distribu-

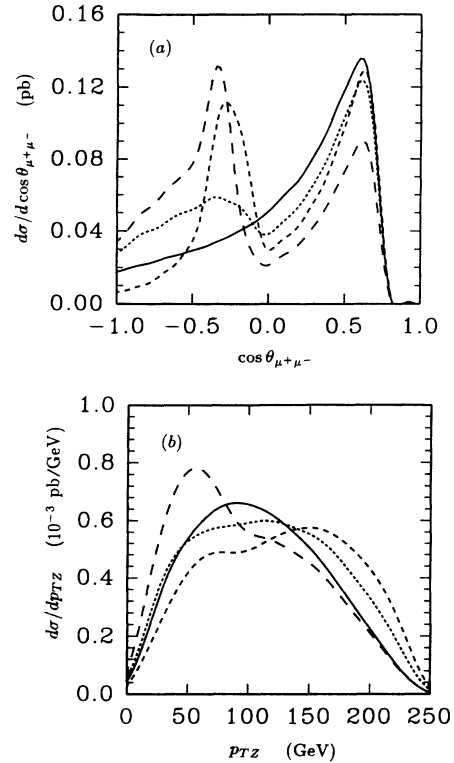


FIG. 4. (a) The angular distribution of the outgoing muons with respect to each other. (b) The transverse-momentum distribution of the reconstructed  $Z^0$ . In both figures the solid line is the standard model prediction, the long-dashed line is for  $\kappa = -0.4$ ,  $\lambda = -0.7$ , the short-dashed line is for  $\kappa = -0.4$ ,  $\lambda = +0.5$ , and the dotted line is for  $\kappa = -1.7$ ,  $\lambda = 0.0$ .

tions to quantify deviations from the standard model, one could choose physics cuts that would optimize the sensitivity to anomalous observations.

If deviations from the standard model were found, the additional information in the distributions would be crucial to determine the values of  $\kappa_Z$  and  $\lambda_Z$ . For example, if  $\kappa_Z$  and  $\lambda_Z$  turned out to be  $-0.5$  and  $-0.8$ , respectively, values of  $\kappa_Z = -0.5$  and  $\lambda_Z = 0.5$  or  $\kappa_Z = -1.5$ ,  $\lambda_Z = -0.25$  would be excluded at better than 99.99% C.L.

#### IV. SUMMARY

We have examined how well the  $WWZ^0$  trilinear gauge-boson coupling could be determined at a  $\sqrt{s} = 500 \text{ GeV}$   $e^+e^-$  collider and have demonstrated how the  $WWZ^0$  vertex can be measured *nearly independently* of the  $WW\gamma$  vertex. We have shown that varying only one parameter at a time can lead to misleading conclusions. The measurement of the cross section by itself would lead to  $0.6 < \kappa_Z < 1.3$  and  $-0.6 < \lambda_Z < 0.4$  when varying one parameter at a time (with  $2 \text{ fb}^{-1}$ ) while it leads to a broad ellipse in parameter space that extends from  $-2.0 < \kappa_Z < 1.5$  to  $-1 < \lambda_Z < 0.8$ . By considering the angular distribution of the two leptons with respect to each other and the transverse momentum of the  $Z$  boson,

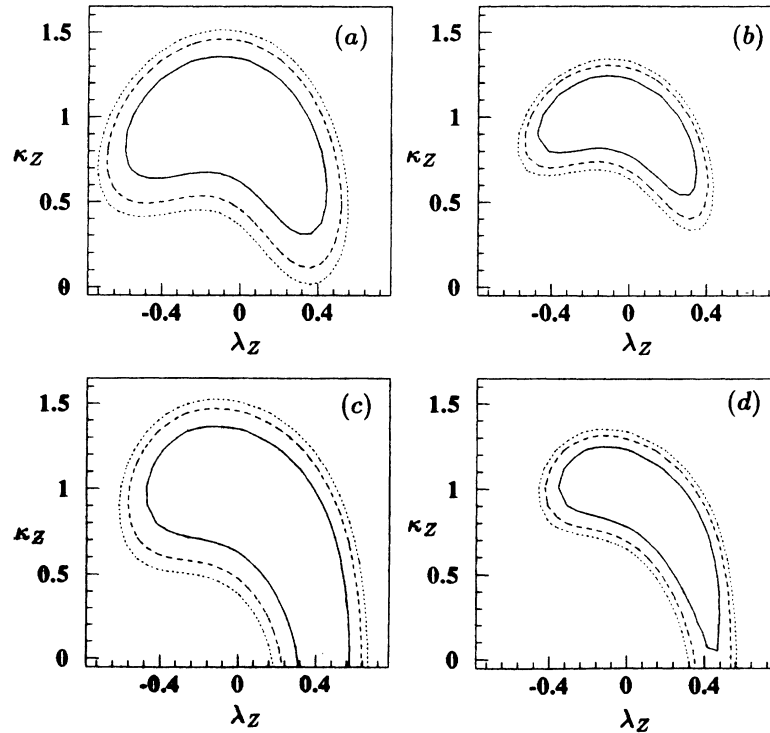


FIG. 5. Confidence-level contours for consistency with the standard model as a function of  $\kappa_Z$  and  $\lambda_Z$  (a) based on the angular distribution of the  $\mu^+$  and  $\mu^-$  with respect to each other for integrated luminosity of  $2 \text{ fb}^{-1}$ , (b) for  $5 \text{ fb}^{-1}$ , (c) based on the transverse momentum distribution of the reconstructed  $Z^0$  for  $2 \text{ fb}^{-1}$ , (d)  $5 \text{ fb}^{-1}$ . In all cases the solid line is the 68% C.L., the dashed line is the 90% C.L., and the dotted line is the 95% C.L.

this ellipse is substantially reduced to  $0.0 < \kappa_Z < 1.5$  and  $-0.6 < \lambda_Z < 0.5$ . As such, the NLC would be a valuable tool in disentangling the  $WWZ^0$  vertex from the  $WW\gamma$  vertex.

The process at hand is richer than the results we just mentioned. Indeed, the most dramatic effects of anomalous gauge-boson couplings do not appear at the poles but as interference between the photon and  $Z^0$  away from either resonance. We found that in the regions  $25 \text{ GeV} < M_{\mu^+\mu^-} < 86 \text{ GeV}$  and  $96 \text{ GeV} < M_{\mu^+\mu^-} < 500 \text{ GeV}$  the interference between the photon and the  $Z$  boson leads to sizable effects when varying  $\kappa_\gamma$  or  $\lambda_\gamma$  in addition to  $\kappa_Z$  and  $\lambda_Z$  [8]. Thus, at the  $Z$ -boson pole, one can measure  $\kappa_Z$  and  $\lambda_Z$  and off the  $Z^0$  pole, one can also observe deviations in  $\kappa_\gamma$  and  $\lambda_\gamma$ . For example, using the  $M_{\mu^+\mu^-}$  bins,  $25 \text{ GeV} < M_{\mu^+\mu^-} < 86 \text{ GeV}$ ,  $86 \text{ GeV} < M_{\mu^+\mu^-} < 96 \text{ GeV}$ ,  $96 \text{ GeV} < M_{\mu^+\mu^-} < 110 \text{ GeV}$ , and  $110 \text{ GeV} < M_{\mu^+\mu^-} < 400 \text{ GeV}$ , we found that at 95% C.L.

$\Delta\kappa_Z = {}^{+0.13}_{-0.7}$ ,  $\Delta\lambda_Z = \pm 0.07$ ,  $\Delta\kappa_\gamma = {}^{+0.21}_{-0.07}$ , and  $\Delta\lambda_\gamma = {}^{+0.08}_{-0.10}$  varying one parameter at a time. However, as we saw above, one should be cautious how one interprets the results when varying only one parameter at a time. Nevertheless, the NLC offers the possibility of measuring all four  $C$ - and  $P$ -conserving parameters of a general  $VWW$  vertex. A complete analysis is in progress and will be presented elsewhere [19].

#### ACKNOWLEDGMENTS

This research was supported in part by the Natural Science and Engineering Research Council of Canada. G.C. thanks the Superconducting Supercollider Center, TRIUMF, and the I.S.E.M. at S.M.U. for the use of their computing facilities. S.G. and R.L. thank the University of Toronto ZEUS and CDF Collaborations and the University of Guelph for the use of their computing facilities.

- [1] S. L. Glashow, Nucl. Phys. **22**, 579 (1961); S. Weinberg, Phys. Rev. Lett. **19**, 1264 (1967); A. Salam, in *Elementary Particle Theory: Relativistic Groups and Analyticity (Nobel Symposium No. 8)*, edited by N. Svartholm (Almqvist and Wiksell, Stockholm, 1968).
- [2] G. Altarelli, in *Proceedings of the XIVth International Symposium on Lepton and Photon Interactions*, Stanford,

- California, 1989, edited by M. Riordan (World Scientific, Singapore, 1990), p. 286; C. Jarlskog, in *Proceedings of the XXVth Conference on High Energy Physics*, Singapore, 1990, edited by K. K. Phua and Y. Yamaguchi (World Scientific, Singapore, 1991).
- [3] U. Amaldi *et al.*, Phys. Rev. **D 36**, 1385 (1987); G. Costa *et al.*, Nucl. Phys. **B297**, 244 (1988); P. Langacker, M.

- Luo, and A. K. Mann, University of Pennsylvania Report No. UPR-0458T, 1991 (unpublished).
- [4] M. Samuel *et al.*, Carleton University report, 1990 (unpublished); U. Baur and E. L. Berger, Phys. Rev. D **41**, 1476 (1990), and references therein.
- [5] D. Atwood *et al.*, in *High Energy Physics in the 1990's (Snowmass 1988)*, Proceedings of the Summer Study, Snowmass, Colorado, edited by S. Jensen (World Scientific, Singapore, 1989), p. 264; U. Baur and D. Zeppenfeld, Nucl. Phys. **B325**, 253 (1989); D. Atwood *et al.*, in *Research Directions for the Decade*, Proceedings of the Summer Study, Snowmass, Colorado, 1990, edited by E. L. Berger and I. Butler (World Scientific, Singapore, in press).
- [6] S. Godfrey, Carleton University Report No. OCIP/C 91-3 1991 (unpublished).
- [7] K. Hagiwara *et al.*, Nucl. Phys. **B282**, 253 (1987); D. Zeppenfeld, Phys. Lett. B **183**, 380 (1987); D. Treille *et al.*, in *Proceedings of the ECFA Workshop on LEP 200*, Aachen, West Germany, 1986, edited by A. Böhm and W. Hoogland (CERN Report No. 87-08, Geneva, Switzerland, 1987), Vol. 2, p. 414. D. A. Dicus and K. Kallianpur, Phys. Rev. D **32**, 35 (1985); M. J. Duncan and G. L. Kane, Phys. Rev. Lett. **55**, 773 (1985).
- [8] G. Couture, S. Godfrey, and R. Lewis, in *Research Directions for the Decade* [5].
- [9] See, for example, T. L. Barklow, in *Research Directions for the Decade* [5]; M. E. Peskin, in *Proceedings of the SLAC Summer Institute on Particle Physics*, Stanford, California, 1987, edited by E. Brennan (SLAC, Stanford, 1987); G. J. Feldman, in *Collider Physics: Current Status and Future Prospects*, Proceedings of the Eighth Vanderbilt High Energy Physics Conference, Nashville, Tennessee, 1987, edited by R. S. Panvini and J. Brau (World Scientific, Singapore, 1988).
- [10] K. Gaemers and G. Gounaris, Z. Phys. C **1**, 259 (1979); K.-i. Hikasa, Phys. Rev. D **33**, 3203 (1986); K. Hagiwara *et al.*, Nucl. Phys. **B282**, 253 (1987); J. Fleischer *et al.*, Z. Phys. C **42**, 409 (1989).
- [11] G. Couture and J. N. Ng, Z. Phys. C **35**, 65 (1987).
- [12] G. Couture *et al.*, Phys. Rev. D **38**, 860 (1988), and references therein.
- [13] U. Baur and D. Zeppenfeld, Phys. Lett. B **201**, 383 (1988); C. Bilchak *et al.*, Report No. CERN-TH.4823/87, 1987 (unpublished) J. M. Cornwall, D. N. Levin, and G. Tiktopoulos, Phys. Rev. Lett. **30**, 1268 (1973); Phys. Rev. D **10**, 1145 (1974); C. H. Llewellyn Smith, Phys. Lett. B **46**, 233 (1973); S. D. Joglekar, Ann. Phys. (N.Y.) **83**, 427 (1974).
- [14] A. Grau and J. A. Grifols, Phys. Lett. **154B**, 283 (1985); P. Mery *et al.*, Z. Phys. C **46**, 229 (1990).
- [15] G. Kane, J. Vidal, and C. P. Yuan, Phys. Rev. D **39**, 2617 (1989).
- [16] G. Belanger *et al.*, Phys. Rev. Lett. **65**, 2943 (1990).
- [17] R. Kleiss and W. J. Stirling, Nucl. Phys. **B262**, 235 (1985); Z. Xu, D.-H. Zhang, and L. Chang, Nucl. Phys. **B291**, 392 (1987); see also G. Couture, S. Godfrey, and P. Kalyniak, Phys. Rev. D **39**, 3239 (1989), for a summary of the method used here.
- [18] See, for example, V. Barger and R. Phillips, *Collider Physics* (Addison-Wesley, Reading, MA, 1987).
- [19] G. Couture and S. Godfrey, Carleton University Report No. OCIP/C 91-7, 1991 (unpublished).